Langit Biru: Jurnal Ilmiah Aviasi Vol. 17 No. 01 Month February Page. 23 : 33
ISSN (p) 1979-1534 ISSN (e) 2745-8695

ANALYZING AERODYNAMIC PERFORMANCE OF TWO-DIMENSIONAL NACA 642415 USING XFLR5 APPLICATION: A RESEARCH BASELINE

Sukahir[(1)], Nukman[(2)], Irsyadi Yani[(3)]
[1]Palembang Aviation Polytechnic
[2,3]Engineering Study Program, Doctoral Program of Engineering Faculty, Universitas Sriwijaya
Corresponding: sukahir@poltekbangplg.ac.id

Received :	Revised :	Accepted :
06 February 2024	01 March 2024	20 May 2024

Abstract: A research baseline is necessary for researchers who would like to conduct follow-up research in the future. Apart from experiments, simple numerical simulations can be used to briefly compare the aerodynamic performance of airfoils and wings of aircraft and UAVs. This research showed the aerodynamic performance of NACA 642415 using the XFLR5 application with an angle of attack $\alpha = 0^o, 2^o, 4^o, 6^o, 8^o, 10^o, 12^o, 14^o, 16^o, 18^o$, and 20^o. The application can briefly and quickly show the aerodynamic performance of airfoils and wings. Then, the pressure coefficient can concisely show the separation point and stall point that occurs even though it cannot be shown directly through the lift coefficient results.
Keywords: airfoil, NACA 642415, XFLR5, pressure coefficient, lift coefficient

Introduction

Airfoils greatly determine the aerodynamic performance of the airplane wings. The use of different airfoils will result in different aerodynamic performance. Therefore, choosing the right airfoil is crucial because most of the lifting force on the aircraft is created on the wings. One type of airfoil variant is the National Advisory Committee for Aeronautics (NACA) series. The NACA series in aircraft includes many shapes, including wings and turbines. Using airfoils with four-digit, five-digit, and six-digit NACA certainly results in different performance.

Various studies have been conducted to improve the aerodynamic performance of aircraft wings. One of them emphasized the selection of the right airfoil for the right type of aircraft. Each aircraft manufacturer will choose an airfoil that is unique to the aircraft they produce. For this reason, the aerodynamic performance of each aircraft will differ depending on the specifications set by each aircraft manufacturer. Proper aerodynamic testing is required as a research baseline for each airfoil. Currently, there are many applications used in aircraft performance testing. Some applications that are widely used by researchers include Ansys, Star CCM, Autodesk CFD, and others.

Researchers have also used those applications as one of the tools for their research on aircraft performance, including Aprovitola et al. (2022), Chinnappa and Srinivas (2023), Fernando and Mudunkotuwa (2021), Hızalan et al. (2023), Ismeal et al. (2024), Islas-Narvaez et al. (2023), Kusuma et al. (2023), and Thomas et al. (2023). In addition, the applications are also used in UAV analysis (Almallah et al., 2023; Hariyadi, Sutardi, & Widodo, 2018; Hariyadi et al., 2018; Hariyadi et al., 2019; Putro et al., 2019; Hariyadi, Sutardi, Widodo, & Mustaghfirin, 2018; Hariyadi, Sutardi, Widodo, & Rachmadiyan, 2018). On the other hand, several researchers used the XFLR5 application in analyzing aerodynamic performance (Communier et al., 2015; Guzelbey et al., 2018; Kakade et al., 2022; Lesalli & Cahyono, 2020; Prasetyo et al., 2023; Yang et al., 2023).

DOI: https://doi.org/10.54147/langitbiru.v17i01

One of the aerodynamic-related studies in Indonesia is that conducted by Hariyadi et al. (2018). They examined the aerodynamic performance of the Eppler 562 wing through numerical studies. Ansys was employed as the application using the k-Ω SST turbulent model. They employed freestream velocity at 10 m/s with plain wing and forward and rearward wingtip fence variations on the UAV. Their study found that induced drag mostly contributes to the formation of total drag and the forward wingtip fence configuration can reduce it better than other configurations.

Another respected study was conducted by Lesalli and Cahyono (2020). They analyzed the static stability of the Adelaar 2 aircraft model using XFLR5 software. This software can calculate the static stability characteristics of the aircraft and provide visuals, graphs, and simulations of aircraft stability. Adelaar 2 is a UAV with a flying wing configuration and is analyzed using XFLR 5 software. It was analyzed with aircraft mass input with the center of gravity located at 5% of the average aerodynamic chord in front of the neutral point and aircraft geometry types, namely airfoil root, tip, span, winglet geometry, and swept wing. Adelaar 2 was qualified for longitudinal static stability after inputting the XFLR5 parameter, and stability characteristics were obtained for wing angles of attack of 22.5^o, 25^o, 27.5^o, and 30^o.

Finally, Hasan et al. (2022) studied and analyzed the airfoil of a solar energy UAV using XFLR analysis. A UAV weighing 2.98 kg was studied to examine its power calculation, solar cell implementation, and design aspects, including airfoils, fuselage, and tail section. From the analysis, it was found that the flight performance of the UAV at solar radiation intensity above 451.23 W/m^2 for the power system increases battery life and works more efficiently at solar radiation intensity above 666.5 W/m^2.

In this study, the XFLR5 application was used to create a research baseline by showing two-dimensional aerodynamic performance. With the aerodynamic performance of a two-dimensional airfoil, it can be assumed that the most normal condition on the aircraft is at midspan. This research baseline can be used as a comparison for three-dimensional wings or wings equipped with high-lift devices.

Method

Math Model

To calculate aerodynamic performance, this study used the XFLRS application. The application calculated the lift coefficient, drag coefficient, and lift-to-drag ratio. The XFLR5 inviscid analysis in two dimensions has a linear-vorticity flow function formulation. For analysis, the application created an inviscid airfoil flow field in two dimensions. This flow field consisted of not only the freestream flow but also the vortex sheet on the airfoil, along with sources on the wake and airfoil surfaces. The stream function can be expressed as:

$$\psi(x,y) = u_\infty - v_\infty + \frac{1}{2\pi}\int \gamma\,(s) lnr(s\colon x,y)ds + \frac{1}{2\pi}\int \sigma\,(s)\theta(s\colon x,y)ds$$

where σ is the source sheet strength, γ is the vortex sheet strength, s is the coordinate through the vortex and source sheet, $v_\infty = q_\infty sin\alpha$ and $u_\infty = q_\infty cos\alpha$ is the freestream velocity components, r is the vector magnitude between the field points x, y and point s and θ is the angle vector (Guzelbey et al., 2018).

For viscous flow analysis with known airfoil geometry, the XFLR5 provides solutions for airfoil surface vortices by solving matrix equations and Kutta conditions. It used Gaussian elimination as follows:

$$\gamma_i = \gamma_{0i} Cos\alpha + \gamma_{90i} Sin\alpha + \sum_{j=1}^{N+N_w-1} (b'_{ij}\alpha_{0,j})\,;1 \le i \le N$$

where γ_0 and γ_{90} are the vorticity distributions, which are free flow α of 0 and 90 degrees. $b'i,j$ = α-1i,jbi,j is the source influence matrix. For viscous flow, the boundary layer equation must be added to γi = qi to obtain a solvable closed system since the source strength is unknown.

Aerodynamic Performance Parameters

An object moving through a fluid causes two forces to form, often called drag and lift. The lift force is perpendicular, and the drag force is parallel to the direction of relative airflow. In general, lift, drag, and pitching moment are expressed in the following equation:

$$L = \frac{1}{2}\rho V^2 C_L$$

$$D = \frac{1}{2}\rho V^2 C_D$$

$$M = \frac{1}{2}\rho V^2 C_M c$$

where L is lift, M is pitching moment, D is drag, A is reference area, c is chord length, V is velocity, ρ is fluid density and CL, CM and CD are lift coefficient, pitching moment and drag coefficient, respectively (Anderson, 2012). In addition, to show the occurrence of the separation point on the airfoil, it is necessary to pay attention to the visualization of the pressure coefficient. The pressure coefficient is defined as:

$$C_p = \frac{P - P_\infty}{\frac{1}{2}V^2} = 1 - \left(\frac{v}{v_\infty}\right)^2$$

(Houghton et al., 2013)

Research Model

This research used numerical simulations on NACA 642415 airfoil in two-dimensional form. It employed a free version of XFLR5. XFLR5 is an aerodynamic application that analyzes airfoils, wings, and aircraft, especially at low Reynolds Numbers. NACA 642415 airfoil in two-dimensional form, as presented in Figure 1.

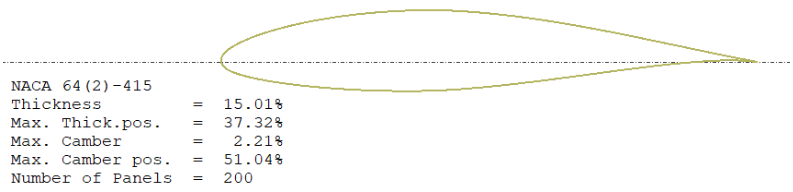

Figure 1. NACA 642415 airfoil

In this research, the XFLR5 application was operated in several stages. First, the NACA 642415 airfoil should be refined prior to running the application. The refined NACA airfoil is illustrated in Figure 2.

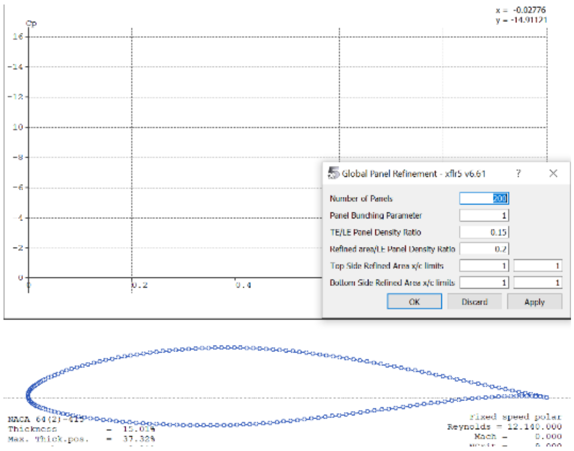

Figure 2. Refining NACA 642415 Airfoil on XFLR5

Further, an analysis was defined using Type 1, namely constant Re. As shown in Table 3, running was done at Re = 12,14 x 10^6.

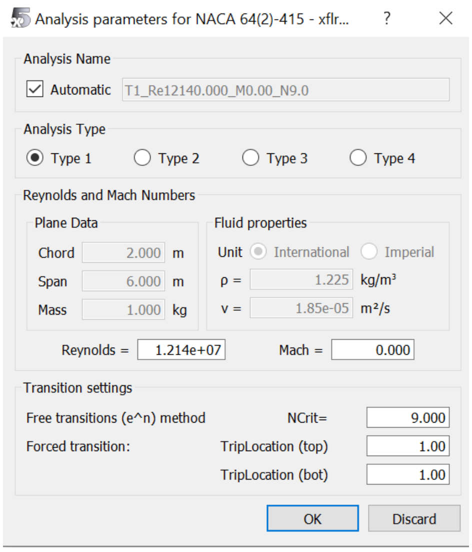

Figure 3. Defining an analysis of NACA 642415 Airfoil on XFLR5

After that, the foil analysis was directed at an angle of attack α = 0º-20º with an interval of 1 degree, as shown in Figure 4.

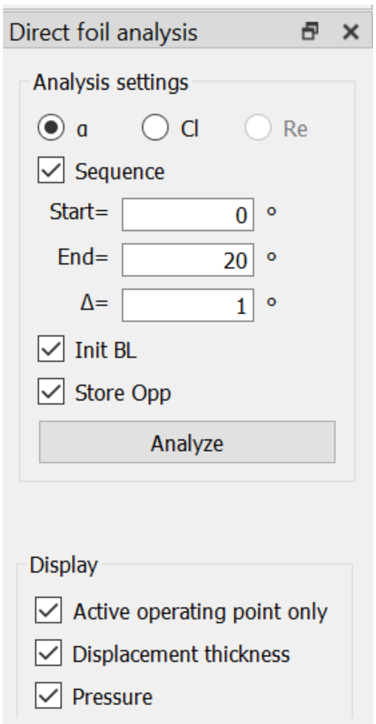

Figure 4. Directing foil analysis of NACA 642415 airfoil on XFLR5

To validate the application of XFLR% in this research, a comparison was made with the experimental results conducted by Ananda and Selig (2016) at Re = 3.45 x 10^6. The C_L calculation showed that the separation occurred with a constant upper surface value at the angle of attack α = 16°. Therefore, the results obtained from the XFRL5 application were valid to be analyzed and presented.

Result

This section is divided into two parts. The first part discusses the results of the pressure coefficient on the upper and lower surfaces. It is then followed by presenting the results of drag and lift coefficient.

Pressure Coefficient (Cp)

When air passes through an airfoil, the local velocity around the airfoil changes. According to Bernoulli's theory, when this happens, the static pressure changes. The pressure distribution determines the lift, pitching moment, resistance of the wing profile shape, and the location of the center of pressure. Pressure is usually expressed as a pressure coefficient. The pressure coefficient (Cp) is the difference between the local pressure measurement and the free flow pressure divided by the dynamic pressure.

One of the results of the XFLR5 application is the visualization of the pressure coefficient on the upper and lower surfaces. As shown in Figure 5, the pressure difference between the lower and the upper surfaces starts moving in the negative y direction, starting from the angle of attack α = 2°. At an angle of attack of α = 6°, the upper surface has perfectly negative values in all parts, while the lower surface is always positive. Also, at the angle of attack α = 6°, the thickness of the boundary layer starts to be clearly visible until the next angle of attack.

In the pressure visualization, at the angle of attack α = 0°-6°, there is no specific increase in the leading-edge area. After the angle of attack α = 6°, the pressure increases on the leading-edge side and is clearly visible along with the increase in the next angle of attack.

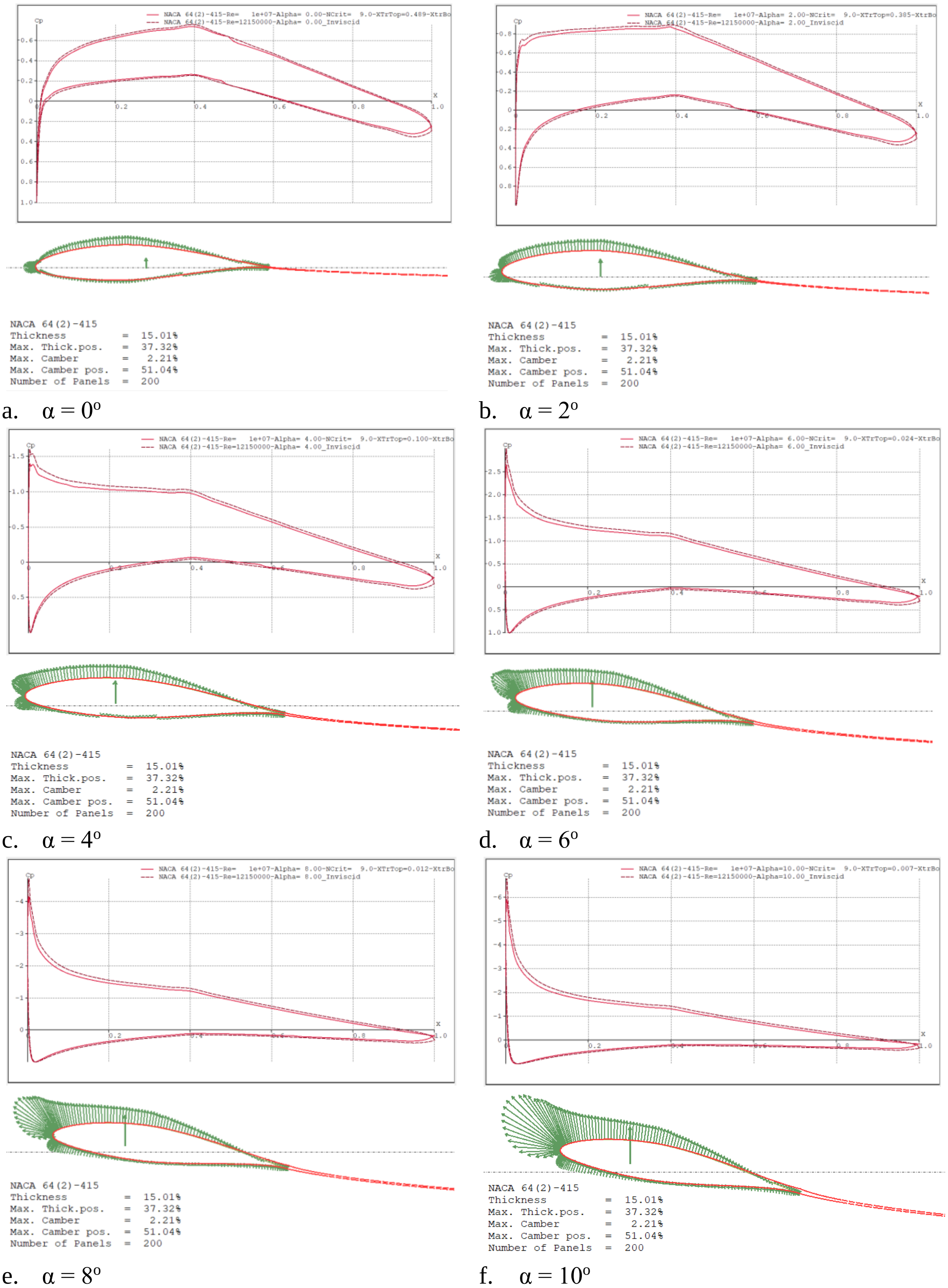

Figure 5. Visualization of pressure coefficients on the upper and lower surfaces of NACA 642415 airfoil at angle of attack α = 0°-10°

Figure 6 shows the visualization of the pressure coefficient on the upper and lower surfaces of the NACA 642415 airfoil at an angle of attack α = 12°-18°. At an angle of attack α = 12°-18°, the upper surface gradually shows a horizontal line where the flow separation begins to occur. At this angle, the pressure difference between the upper and lower surfaces is becoming more constant. At the leading edge, the pressure that arises has almost the same value, while the boundary layer at the trailing edge is getting thicker.

This finding shows that the longer separation flow begins to advance closer to the leading edge area, especially when the angle of attack increases. In addition, the separation is characterized by the thickening of the boundary layer at the trailing edge as the angle of attack increases.

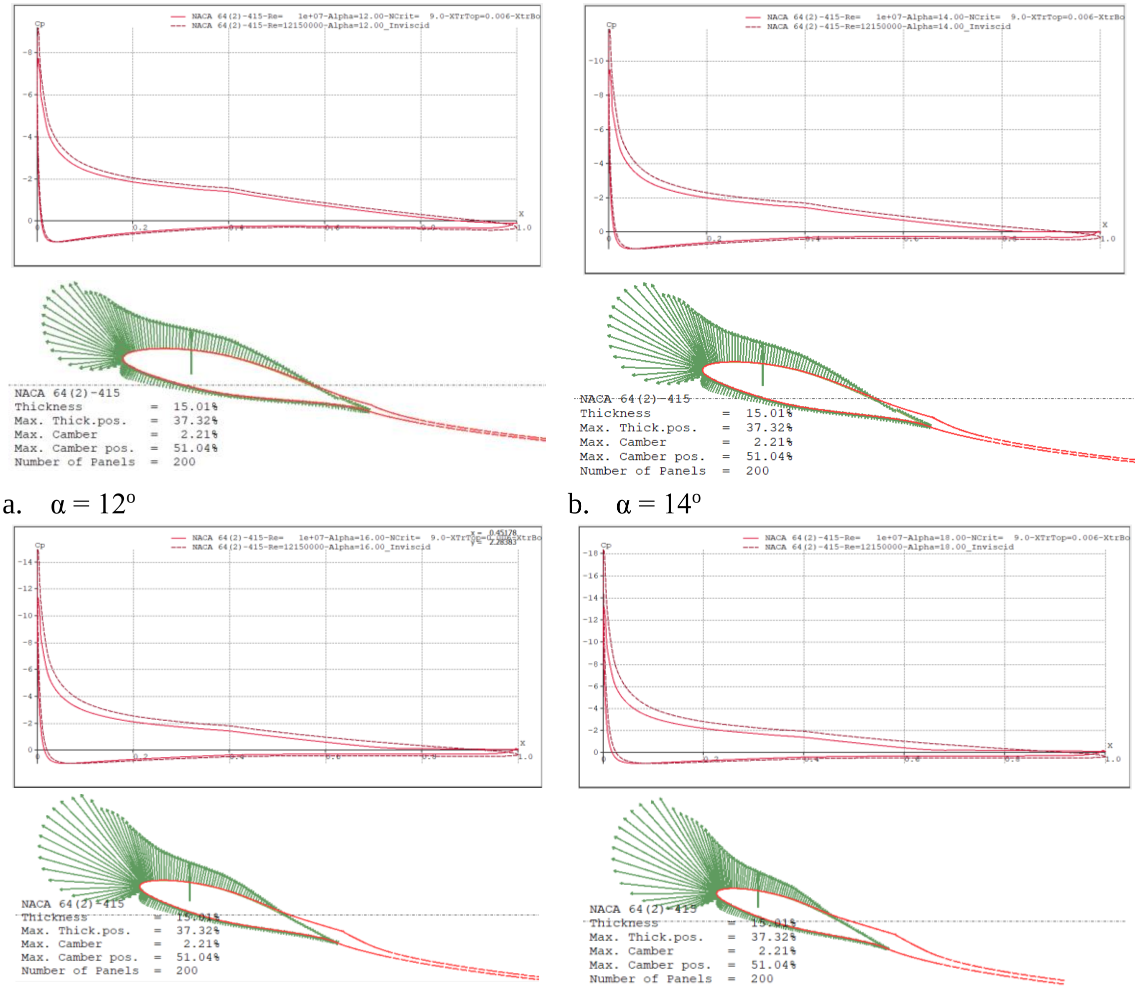

a. α = 12°
b. α = 14°
c. α = 16°
d. α = 18°

Figure 6. Visualization of pressure coefficients on the upper and lower surfaces of NACA 642415 airfoil at angle of attack α = 12°-18°.

Drag and Lift Coefficient

Figure 7 shows the results of the lift and drag coefficients at the angle of attack α = 10°-18°. Explicitly, the figure compares the lift and drag coefficient. However, it does not provide the lift-to-drag ratio because it must be recalculated. Figure 7 shows the comparison of lift and drag as the angle of attack increases. However, the lift coefficient cannot show the precise angle of attack where the stall occurs. Likewise, the drag coefficient cannot show how the influence of each component forms the drag coefficient.

ISSN (p) 1979-1534 ISSN (e) 2745-8695

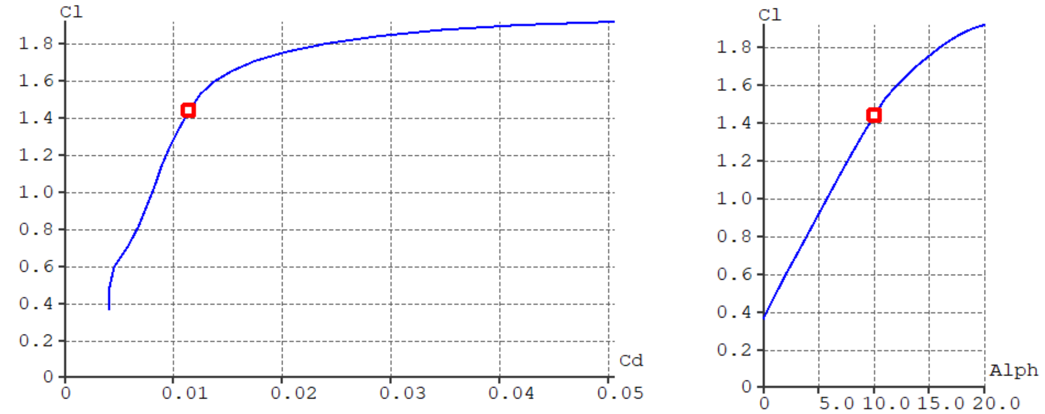

a. α = 10º

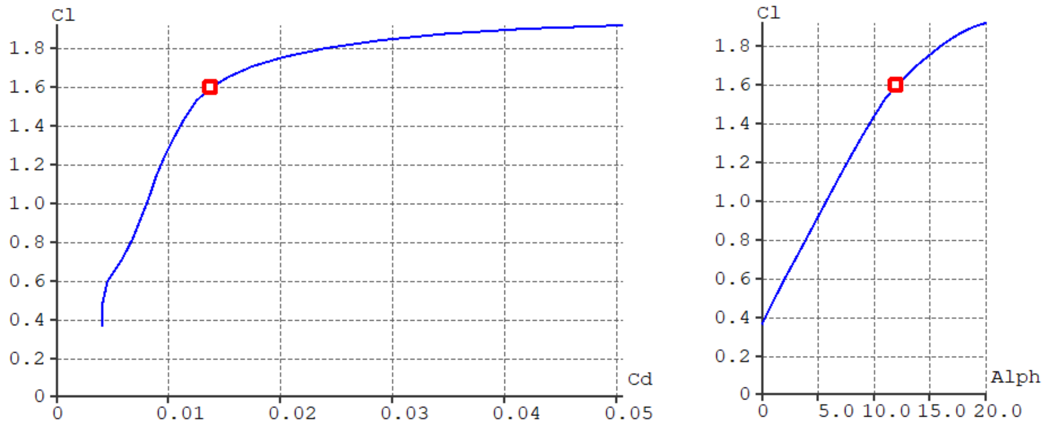

b. α = 12º

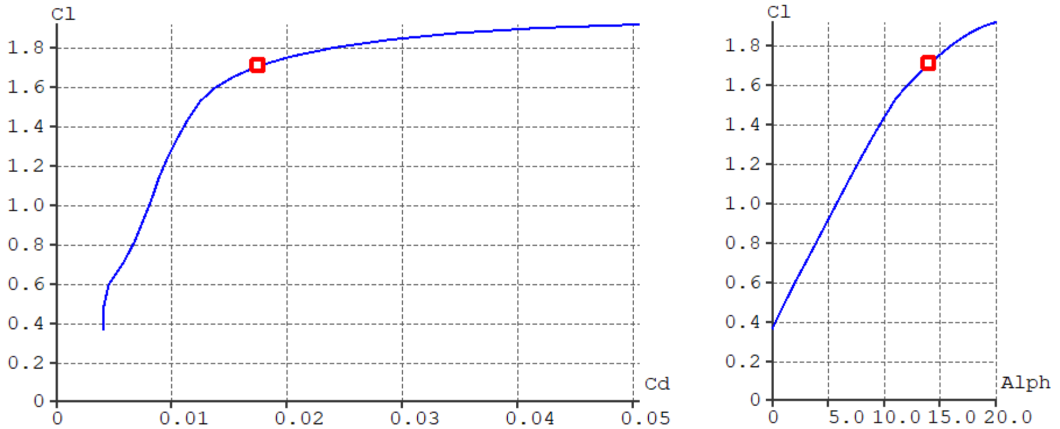

c. α = 14º

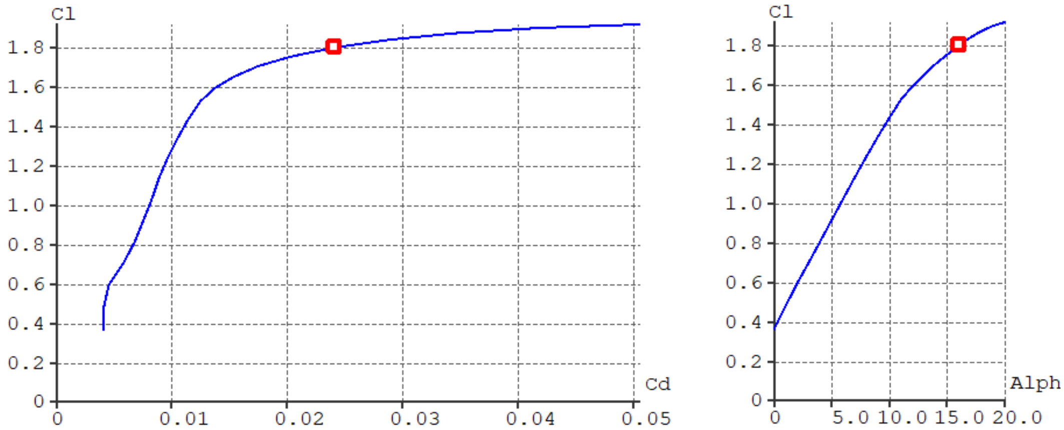

d. α = 16º

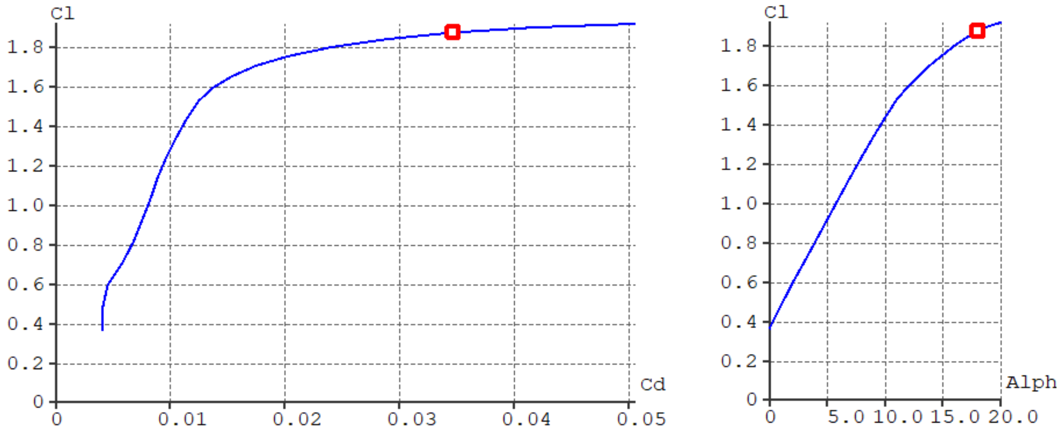

e. α = 18º

Figure 7. Visualization of lift and drag coefficients of NACA 642415 airfoil at several angles of attack α = 10º-18º

Discussion

This research analyzes the aerodynamic performance of the two-dimensional NACA 642415 using the XFLR5 application. The application can show the results of two-dimensional numerical simulation objects on the NACA 642415 airfoil in detail, especially on the pressure coefficient (Cp). It can also show the approximate thickness of the boundary layer. The increase in pressure coefficient at the leading edge is shown in the visualization simulation image. In this research, the pressure increases as the angle of attack increases.

The occurrence of separation can be seen from the constant value of the pressure coefficient at the upper surface. However, the occurrence of stall cannot be seen directly in the image of the lift coefficient results. Similarly, the results of the pressure coefficient cannot directly show the components that form the drag coefficient, such as viscous drag, pressure drag, and induced drag (Gudmundsson, 2013).

This research was conducted in a two-dimensional simulation that has limitations on the observation area on the upper and lower surfaces of the airfoil. In reality, the pressure difference is uneven in certain parts. Thus, the observation is generally carried out at the midspan part of the wing. Examples of uneven pressure differences have been shown in earlier research (Hariyadi et al., 2022; Putro et al., 2022, 2024).

Furthermore, the XFLR5 application is also limited to having a database on certain NACA-type airfoils. In reality, there are still many types of airfoils used in aircraft that do not use NACA-type airfoils. In addition, the output of the XFLR5 still needs to be compared with the results of research using other applications or experiments to get accurate results. Still, the XFLR5 alone is sufficient to provide a brief overview of the aerodynamic performance of the wing.

Conclusion

Numerical simulations have been carried out using the XFLR5 application. The results of this study can be used as a valid baseline because they have been compared with the results of other studies. The pressure coefficient can be shown precisely and accurately in the two-dimensional analysis. Some shortcomings can be seen with the designation of the lift coefficient results that have not been able to show the stall point and the designation of the drag coefficient component.

Further research can be carried out using a simple three-dimensional analysis of a particular wing shape. The three-dimensional analysis can show the use of wings under certain conditions. Variations in wing shape can show the actual performance of the analyzed aircraft coupled with vertical and horizontal stabilizer components in addition to the body of the aircraft that can be added.

Acknowledgments

The authors would like to extend their deep gratitude to the Palembang Aviation Polytechnic for financially supporting this research through their research grant scheme.

Bibliography

Akhil P Thomas, Nandu S Nair, Abin Jose, & Neethi Madhavan CS. (2023). Design and Analysis of Flexible Wing. *ACS Journal for Science and Engineering*, *3*(1), 42–52. https://doi.org/10.34293/acsjse.v3i1.60

Almallah, S. H., Elnady, A. O., & Okasha Elnady, A. (2023). CFD Analysis of Full Quadcopter. *International Journal of Advanced Multidisciplinary Research and Studies*, *2*(December 2022), 599–604. https://www.researchgate.net/publication/365999969

Aprovitola, A., Dyblenko, O., Pezzella, G., & Viviani, A. (2022). Aerodynamic Analysis of a Supersonic Transport Aircraft at Low and High Speed Flow Conditions. *Aerospace*, *9*(8). https://doi.org/10.3390/aerospace9080411

Chinnappa, V., & Srinivas, G. (2023). Numerical investigation of Aerodynamic Characteristics of NACA 23112 Using Passive Flow Control Technique–Gurney Flaps. *Cogent Engineering*, *10*(1), 1–19. https://doi.org/10.1080/23311916.2023.2222566

Fernando, V. N., & Mudunkotuwa, D. Y. (2021). Bio-Inspired Aircraft Wing Modification Analysis in ANSYS Fluent. *2021 10th International Conference on Information and Automation for Sustainability, ICIAfS 2021*, *August*, 316–321. https://doi.org/10.1109/ICIAfS52090.2021.9605821

Hariyadi, S. S. P., Sutardi, & Widodo, W. A. (2018). Drag reduction analysis of wing airfoil E562 with forward wingtip fence at cant angle variations of 75°and 90°. *AIP Conference Proceedings*, *2001*. https://doi.org/10.1063/1.5049994

Hariyadi, S., Sutardi, S., Widodo, W. A., & Junipitoyo, B. (2019). *Numerical Study of the Wingtip Fence on the Wing Airfoil E562 with Fence Height Variations*. *October*, 16–17.

Hızalan, O., Topçam, A. M., Özsunar, S., Doğan, S., & Ödemiş, A. (2023). Vibratory and Static Analysis of AIRBUS A300 Airplane Wing Model using ANSYS Workbench. *IES 22 International Engineering Symposium*, *January*, 11.

Islas-Narvaez, E. A., Ituna-Yudonago, J. F., Ramos-Velasco, L. E., Vega-Navarrete, M. A., & Garcia-Salazar, O. (2023). Design and Determination of Aerodynamic Coefficients of a Tail-Sitter Aircraft by Means of CFD Numerical Simulation. *Machines*, *11*(1), 1–24.

https://doi.org/10.3390/machines11010017

Ismeal, I. J., Bakirci, M., & Jweeg, M. J. (2024). An Optimum Design of a Subsonic Aircraft Wing due to the Aerodynamic Loading. *Hindawi The Scientifc World Journal*, *2024*, 13.

Kusuma, Y. F., Defianti, H., & Syamsuar, S. (2023). The Effect of Adding Floaters to Airplane Models on Aerodynamic Characteristics Using Computational Fluid Dynamics Methods. *AIP Conference Proceedings*, *2941*(1). https://doi.org/10.1063/5.0181446

Putro, S. H. S., Sutardi, & Widodo, W. A. (2019). *Numerical study of three-dimensional flow characteristics around the wing airfoil E562 with forward and rearward wingtip fence*. 020017. https://doi.org/10.1063/1.5138272

Rudresh, M., Sudhagara Rajan, S., Prashanth, K. P., Vasist, A. S., Dhaduk, D., Deshmukh, S., & Sahoo, S. (2023). Design and Development of a Flying Wing Reconnaissance UAV. *Journal of Engineering Science and Technology*, *18*(5), 2615–2630.

Setyo Hariyadi, S. P., Sutardi, & Widodo, W. A. (2018). Numerical study of flow characteristics around wing airfoil Eppler 562 with variations of rearward wingtip fence. *AIP Conference Proceedings*, *1983*. https://doi.org/10.1063/1.5046207

Setyo Hariyadi, S. P., Sutardi, Widodo, W. A., & Mustaghfirin, M. A. (2018). Aerodynamics Analysis of the Wingtip Fence Effect on UAV Wing. *International Review of Mechanical Engineering*, *12*(10), 837–846. https://doi.org/10.15866/ireme.v12i10.15517

Setyo Hariyadi, S. P., Sutardi, Widodo, W. A., & Rachmadiyan, A. (2018). Numerical simulation of airfoil Eppler 562 with variations of whitcomb wingtip devices. *AIP Conference Proceedings*, *1983*. https://doi.org/10.1063/1.5046199